Physics of the Solid State, 2022, Vol. 64, No. 9

02,13

Experimental study of elements of a Josephson traveling-wave parametric amplifier on SQUID chains.

© *R.A. Yusupov, L.V. Filippenko, M.Yu. Fominskiy, V.P. Koshelets*

Kotelnikov Institute of Radio Engineering and Electronics, Russian Academy of Sciences,
Moscow, Russia

E-mail: yusupovrenat@hitech.cplire.ru

Received April 29, 2022
Revised April 29, 2022
Accepted May 12, 2022

The issues of designing a Josephson traveling-wave parametric amplifier (JTWPA) based on a well-established technology of superconducting microcircuits with given and controlled parameters based on high-quality Nb$-$AlO$_x$$-$Nb tunnel junctions are considered. This technology has been adapted and optimized to obtain structures with the required parameters and circuits with large number of tunnel junctions. To advance the technology, the basic elements of a promising JTWPA have been devel-oped, manufactured and studied. In direct current measurements, a number of super-conducting elements parameters were experimentally determined; these parameters are required for designing a JTWPA chips for microwave measurements. An original design of JTWPA based on a chain of SQUIDs in a coplanar line has been developed for implementation using the IRE niobium technology; the parameters of the main elements of the JTWPA have been determined.

Keywords: Josephson travelling-wave parametric amplifiers (JTWPA), Josephson metamaterials (JMM), Josephson junctions (JJs), cold amplifier, coplanar lines, quantum noise, SIS, SQUIDs.

DOI: 10.21883/0000000000

1. Introduction

Currently, there is a growing interest in the development of various quantum devices (qubits, detectors with a quantum level of sensitivity, etc.), which, by their nature, operate at low and ultralow temperatures at frequencies of a few and tens of GHz. To communicate with quantum systems, elements and devices are needed that can operate at ultralow temperatures and enable to control, process and read information, as well as amplify weak high-frequency signals. The practical parameters of linear semiconductor microwave-amplifiers have reached limit values and do not allow for obtaining the bandwidth, amplification and noise required to create qubit readout systems in a quantum computer, axion detectors, intermediate frequency amplifiers for radio astronomical heterodyne receivers, and systems for reading arrays of cryogenic bolometers with frequency division of channels. The use of the Josephson tunnel junctions (JJ) enables to implement a lossless non-linear inductance and provides characteristics that are unattainable for dissipative non-linear elements. When implementing the phase-sensitive Josephson amplifier under consideration, it is possible to reduce the noise temperature below the quantum limit in the mode of compression of quantum states. It is assumed that the development of a fundamentally new type of broadband microwave traveling wave amplifier will enable to bypass the bandwidth and dynamic range limitations that exist for a traditional lumped-element parametric amplifier and will enable to reduce noise below the quantum limit [1].

The Josephson parametric amplifiers [2] are considered the most advanced devices for fine experiments in the field of quantum measurements and quantum information technologies, but have not yet received wide distribution. Interest in these devices increased after the demonstration of a parametric traveling wave amplifier based on the kinetic inductance of a thin superconducting film [3]. However, the greatest attention of research groups in recent years has been attracted by the Josephson parametric amplifiers in the traveling wave mode, which provide a higher amplification per unit length at lower pump power based on chains of high-frequency (HF) or direct current (DC) SCQIDs [4–7]. In contrast to the lumped Josephson parametric amplifiers with a limited amplification band, JPATW provide signal and pump interaction along the entire length of the microstrip line and provide an extension of the bandwidth and dynamic range of the amplifier.

Zorin's article [8] predicted the possibility of creating a Josephson parametric traveling wave amplifier (with the number of elements in the range of 300$-$600), which can provide amplification in the region of 20 dB in the band 4$-$8 GHz (see Fig. 1, a). More recent articles [9] are not so optimistic anymore and speak of achieving amplification of 7$-$10 dB in a wide band with a reasonable number of cells equal to 1175. The first implementation in PTB [10] showed the fundamental possibility of creating this type of amplifier, and its modernization, performed in HYPRES, demonstrated an average amplification of about 10 dB in this band, but with a fairly strong frequency response [11]. A working prototype of such an amplifier based on niobium SIS-junctions was implemented using a technology with a current density of 100 A/cm^2; symmetrical HF SCQIDs with the Josephson junctions with nominal critical current from 4 to 12 μA were studied in this article.

No noise temperature measurements have been made so far, which, according to theory, should be less than 1 K at an operating temperature of 4.2 K. A prototype of such an amplifier operating at millikelvin temperatures and having a noise temperature close to the quantum limit, less than 0.5 K at 8 GHz, has not been implemented.

2. Design and engineering of JPATW

We have developed a symmetrical design of the JPATW line (Fig. 1, *b*) and separate test structures for determining the inductive parameters of the elements. The critical junction current in real samples is determined by a combination of two factors: the first is R_nS — a parameter determined by the tunneling barrier formation conditions; the second is S — the area of the junction itself (it is more convenient to talk about the linear size — the diameter d_j). We have selected a single JJ size with a diameter of $d_j = 2\,\mu$m (round junctions) and a three-layer structure parameter $R_n = 1000\,\Omega/\mu\text{m}^2$. The corresponding critical current is estimated as $I_c = 5.3\,\mu$A, taking into account that Nb is a tightly coupled superconductor and the actually measured critical current (I_c) of junctions is 0.5–0.6 of the current jump at the slot voltage (I_g). The normal resistance of such a junction (R_n) is estimated to be 320 Ω, and the junction capacitance is $C_j = 160$ fF. Reducing the size of the junction would enable to implement a smaller critical current, but for JPATW operation it is critical to create chains of junctions with a small relative spread of critical currents.

To estimate the optimal parameters of the JPATW design based on HF SCQIDs, a calculation program was created in the MathCAD environment. Main parameter of JPATW is dimensionless inductance of SCQID $\beta_L \equiv 2\pi L_g I_c/\Phi_0$ [8], where L_g is the geometric inductance, should be less than unity for the hysteresis-free form of the volt-flux characteristic, and tends to 1 for the optimal amplification of each individual cell. The value of the geometric inductance L_g is determined by the size and geometry of the SCQID loop, but determining the exact values analytically in such circuits is quite a difficult task. In our scheme, SCQIDs of square shape were selected, they are easier to design and calculate, while they provide a fairly dense placement of cells. The SCQID loop width was 4 μm; this line width is reliably and accurately obtained within the scope of the technology used.

For a more accurate numerical calculation of inductances, the InductEx program was used, which had been created for calculating superconducting circuits. The inductances (L_g) calculated in this way turned out to be higher (57 pH) than those calculated using the simple analytical formula $1.25\mu_0 d$ for a square frame (37.5 pH), in which there is a dependence only on the inner size of the loop. To achieve the desired geometric inductance, the calculated side of the square frame was 24 μm. Earth capacitance C_0 should provide an impedance $Z_0 = (L/C)^{1/2}$ of each cell close to 50 Ω to match the transmission lines, and the cut-off frequency $f_0 = (LC)^{-1/2}$ should be low enough. The calculated capacitance per cell should be 23 fF; in the developed design, it is implemented by two symmetrical areas of superconducting layer overlap with coplanar earth conductors.

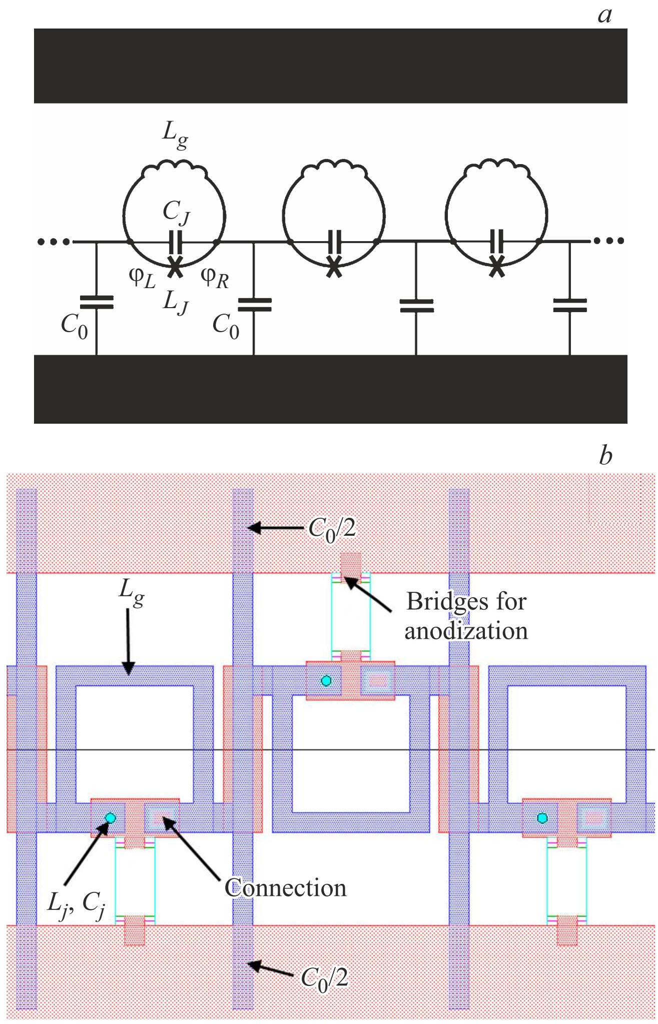

Figure 1. *a*) Electrical diagram of the transmission line, including an array of HF SCQIDs. The Josephson junction is represented as a parallel connection of a Josephson inductance L_j and a tunnel capacitance C_j. *b*) View of the developed line geometry with HF SCQIDs.

For the three-frequency operation mode, for the signal frequency $f_s \sim 0.5 \cdot f_p$, the amplification of the structure of N cells is estimated as $G = \cosh^2(g_0 N)$, where the exponential amplification factor is $g_0 = |\chi|(\beta_L I_p/4I_c) \cdot (f_p/f_0)$. For the calculated amplifier line with $\beta_L = 0.9$, the number of cells to achieve the desired amplification of 20 dB was at least 700 pieces. The parameters for two-terminal direct current SCQIDs, other loop sizes, as well as options with shunted Josephson junctions are calculated similarly.

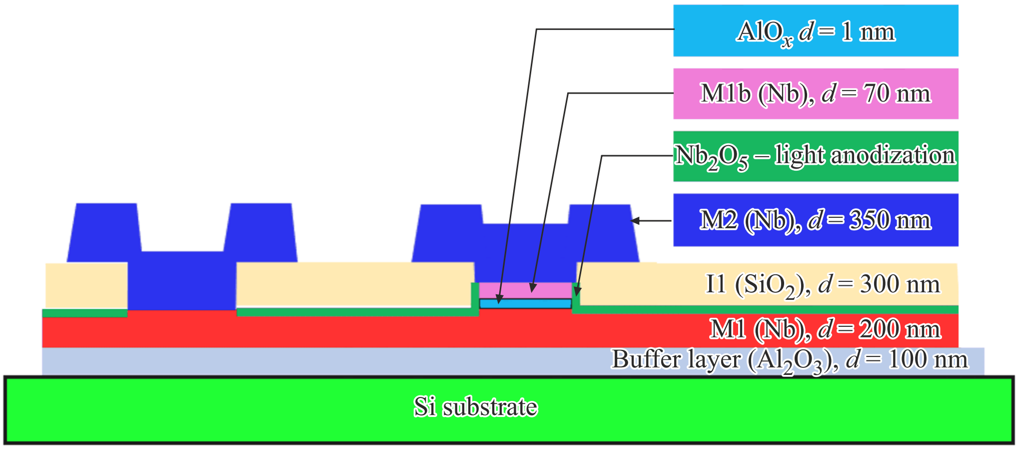

Figure 2. Cross section of an integrated circuit with two superconducting layers.

For the designed SCQID chains, the optimal parameters of the coplanar line in which they are located are calculated. For samples on high-resistance silicon substrates ($\rho > 10\,k\Omega \cdot cm$) 0.5 mm thick, with a metal screen on the reverse side, with metallization thickness of (Nb) of 0.2 μm, center line width of 34 μm, optimal gap to „grounded“ conductors was 19 μm.

3. Technology for manufacturing samples with test structures

A technological complex for manufacture of superconducting structures based on high-quality Nb$-$AlO$_x$$-$Nb tunnel junctions is successfully operating at the Institute of Radio Engineering and Electronics, which enables to obtain structures with a tunnel current density of 0.1 kA/cm^2$\div$10 kA/cm^2 of micron and submicron sizes [12–14]. This technology has been adapted to fabricate samples with two superconducting layers, anodization and an additional insulation layer to reliably prevent short circuits (see Fig. 2). The key requirements for the technology are a relatively low tunneling current density (approximately 0.3 kA/cm^2), the possibility of creating structures with a large number of JJ (up to 1000 pcs.) and small relative spreads parameters of these junctions. Additionally, the possibility of sputtering of shunt resistances for test measurements was laid. Earth capacitance, which is necessary to implement the amplifier line, is proposed to be implemented using insulator layer I1, this capacitance has an estimated value of 0.17 fF/μm^2.

All film sputtering is carried out by magnetron sputtering. First, a thin (100 nm) Al_2O_3 buffer layer is deposited; this sublayer is a stop layer for etching a three-layer structure. Then, in a single cycle, without breaking the vacuum, a three-layer Nb/AlO$_x$/Nb structure is applied, the thicknesses of the corresponding layers are 200, 7 and 80 nm. The geometry of the lower layer of the superconductor was formed using the „explosive photolithography“ (lift-off) method using the M1 mask. The next operation is the formation of the region of tunnel junctions by etching from a three-layer structure using the I1 mask. The same resist mask is used for anodizing, first of all, of the junction walls and sputtering in the areas not covered by the 250 nm thick SiO_2 insulator resist, which provides dusting of the lower electrode to prevent electrical contact between the two superconducting layers. For the contact of two superconducting layers in the desired areas (previously they were also covered with the I1 mask resist), windows are formed by etching using the ETCH mask. The next stage is optional — formation of shunts of Mo, non-superconducting at a temperature of 4.2 K. Shunt junctions are not required in real amplifier structures, and are used only in test structures. The structure of the second superconducting layer (M2) 350 nm thick is formed by the „explosive

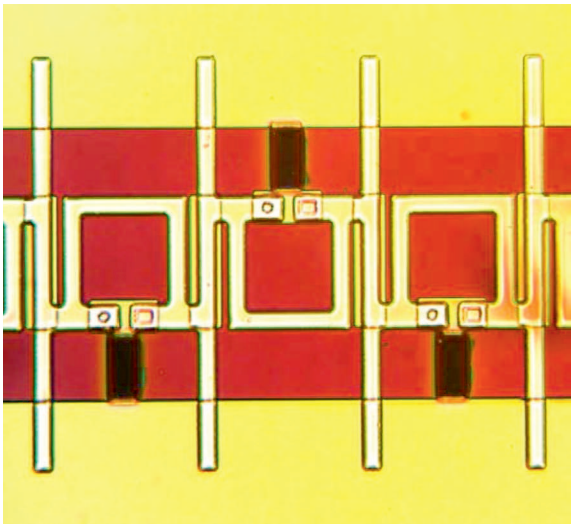

Figure 3. View of the fabricated chain of HF SCQIDs in a coplanar line.

Table 1. Layer film application parameters

Layer	Pattern	Material	Layer description	Thickness, nm
		Al_2O_3	Buffer layer	100
M1	Negative	$Nb/AlO_x/Nb$	Three-layer structure: base electrode Nb, tunneling barrier AlO_x, upper electrode Nb	 200 7 200
I1	Negative	AlO_x/Nb	Formation of the tunneling junction area by the reactive ion etching (RIE) method	80
		Nb_2O_5	Light anodization; 10 V	20
		SiO_2	SiO_2, insulator Capacitance: $0.17\,\mathrm{fF}/\mu\mathrm{m}^2 \pm 25\%$ (Estimation)	300
ETCH	Positive		Etching (Nb and AlO_x) for direct contact M1 with M2 (RIE + KOH)	
M2	Positive	Nb	Nb, superconductor. London penetration depth: $\lambda_L = 85\,\mathrm{nm} \pm 5\%$	350
CONT	Positive	Al/Au	Contact pads	200
ALO	Positive		Final removal of bridges for anodization (RIE)	

Table 2. Measured values of critical currents for JJ of different sizes

d_j, μm	S, μm^2	R_n, Ω	I_g, μA	I_c, μA	I_c/I_g
8.73	59.83	35	74	40	0.54
4.73	17.56	120	21	9.2	0.44
4.23	14.05	150	17	6.8	0.40
3.73	10.92	194	13	4.7	0.36
3.23	8.19	257	10	2.5	0.25
2.73	5.85	349	7	1.5	0.21

lithography“ method. The last process layer is gold contact pads, 200 nm thick, the structure is also created by the „explosive“ lithography method. For better adhesion of gold to niobium, a thin (1–2 nm) aluminum sublayer is used. The last stage is the removal by etching of additional bridges that connected all areas with tunnel junctions for their anodization. All film sputtering parameters are given in Table 1.

Using this technology, two series of samples were made, including individual single DC SCQIDs and chains of HF and DC SCQIDs. For preliminary testing of the fabricated microcircuits containing prototypes of the JPATW elements and evaluation of the junction parameters, three test chips were included in the template, which were fabricated on the same substrate as the working microcircuits. On each test chip, several tunnel SIS-junctions of different area (diameter from 2 to 4 μm) were fabricated.

4. Measurement scheme and measurement results

The measurement results of single test SIS junctions, as well as chains and single DC SCQID at a temperature of 4.2 K are presented. For primary testing, a probe inserted into a transport Dewar with liquid helium was used, which allows for operational testing of fabricated samples. A substrate with the structures under study was attached to the measuring head of the cryogenic probe (14 contact pads were provided), the board with the sample was inside screens made of cryogenic permalloy and superconducting lead. Contacts were made with the help of needles made of beryllium bronze, which has a

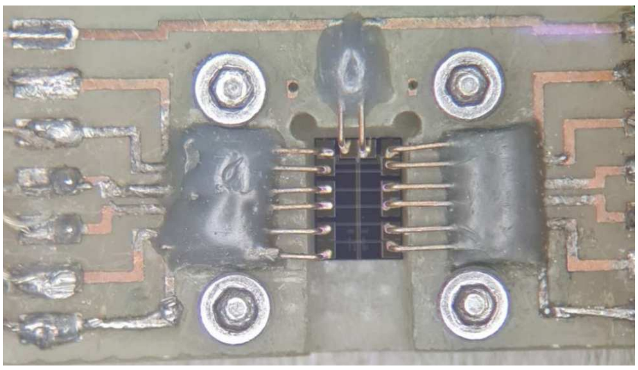

Figure 4. View of the sample holder for preliminary testing of samples at a temperature of 4.2 K.

sufficient degree of elasticity at $T = 4.2\,\mathrm{K}$ (see Fig. 4). Current-voltage characteristics (CVC) were measured using a four-contact circuit. The measurements were carried out both in the voltage setting mode, in order to better describe the features of the current-voltage characteristics at voltages near the gap, and in the current setting mode, in order to more accurately register the critical current of the fabricated SIS-structures. All junctions in all fabricated structures demonstrate high quality, the resistance ratio R_j/R_n of more than 45, and the same gap of $V_g = 2.88\,\mathrm{mV}$ (see Fig. 5), which enables to create high-quality Josephson metamaterials (JMM) using this technology.

In the JPATW circuit based on SCQIDs, the key parameters are the geometric inductance of the SCQID loop and the critical junction current, on which the Josephson inductance depends. In the voltage setting mode with a current jump to normal resistance, there is a so-called knee-shaped feature. For the use of these tunnel structures in JMM, it does not play a role, since the values of the critical current are important. Direct measurements of the critical current in such structures are strongly affected by external magnetic fields and electrical pickups, so the measured values strongly depend on the parameters of the measurement system. For the described measurement system, the values of critical currents were higher in junctions shunted with a small $(10\,\Omega)$ parallel resistance (see Fig. 6). The values of the measured critical current (I_c) turn out to be noticeably smaller than the values of the current jump (I_g) at the target voltage (V_g) of the gap. The theoretical value of I_c/I_g for junctions with strong-coupling superconductors, to which niobium belongs, is $0.5-0.6$. In the measured test transitions, this ratio depended on the junction area and ranged from 0.2 for small junctions to 0.55 for large junctions (see Table 2). First of all, we attribute this to the thermal noise of the SIS-junction, which at a temperature of 4.2 K is $0.4-0.5\,\mu\mathrm{A}$ and the presence of additional interference, which for our non-optimized test system amounted to $1\,\mu\mathrm{A}$. For the junctions with a larger area and high critical currents, these mechanisms played a smaller role.

Fig. 7 shows the results of measuring the test DC SCQID structures, demonstrating the modulation of the critical current and enabling to determine the inductances of the elements under study. The magnetic field in such structures was set by passing direct current through an additional line at a distance of $19\,\mu\mathrm{m}$ from the SCQID loop. The ratio of the maximum and minimum currents per current-of the SCQID flux characteristic depends on the ratio of the geometric and Josephson inductances, and the value of the dimensionless parameter β_L in this measurement was approximately 0.5, which is less than the design value of 0.9. These measurements also demonstrate the possibility of adjusting the SCQIDs line by passing control current through the „grounded“ conductors in a coplanar line.

For chains of SCQIDs, the measured current-voltage characteristics also strongly depend on the configuration of

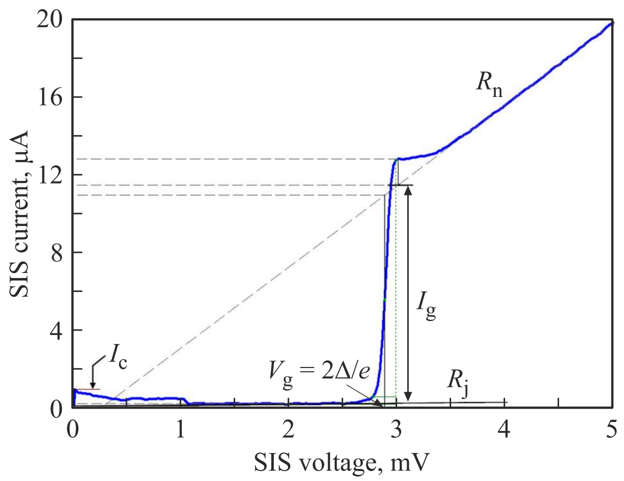

Figure 5. Measured current-voltage characteristic for a single DC SCQID in voltage setting mode with suppressed critical current.

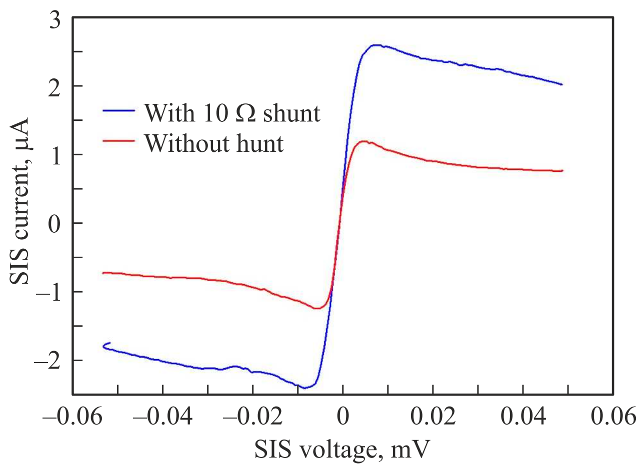

Figure 6. CVC with critical current for a single DC SCQID recorded in the voltage setting mode.

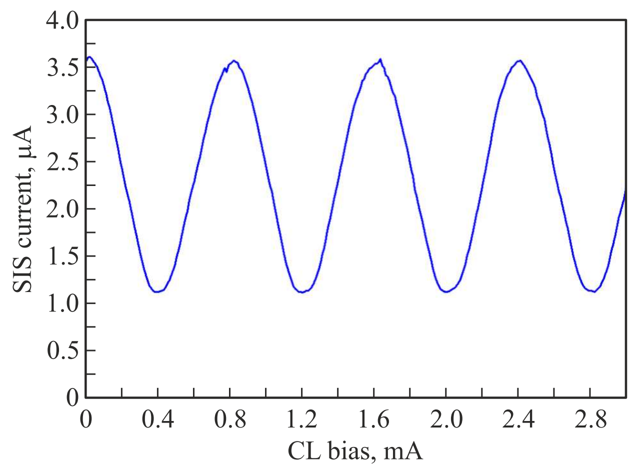

Figure 7. Dependence of current on the magnetic flux through SCQID, given by passing direct current through the control line.

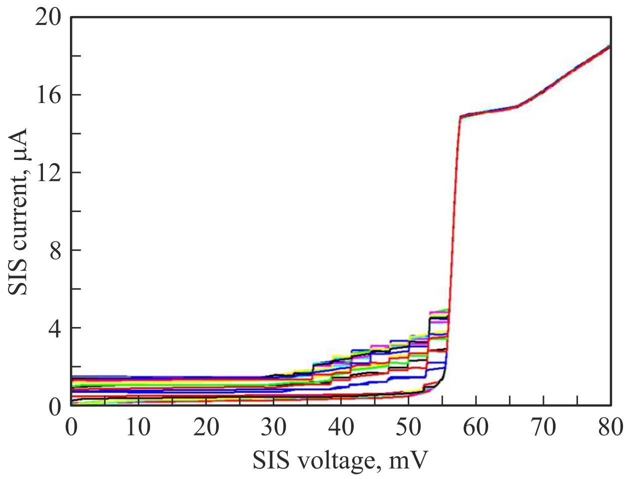

Figure 8. Current-voltage characteristics of a chain of 20 DC SCQIDs taken in the current setting mode at various current values (0−1 mA) in the control line.

the system, which complicates estimation of the parameters of individual cells. As an example, Fig. 8 shows the current-voltage characteristics of a chain of 20 series-connected DC SCQIDs taken with different values of the magnetic field; which leads to variation of the critical current values of individual cells. The measured critical currents for such a chain were up to $3\,\mu$A in terms of one JJ and the ratio $I_c/I_g \approx 0.5$ (excluding the knee-shaped feature just above the slot voltage). Therefore, to design a line based on HF SCQIDs, one can focus on the current values at the slot voltage.

5. Conclusion

The basic elements for the implementation of JPATW based on SCQIDs have been developed and studied. One of the options for the design of such JPATW is a chain of HF SCQIDs in a coplanar line. We have developed an original design of such an amplifier, taking into account the features of the $Nb-AlO_x-Nb$ technology of the Institute of Radio Engineering and Electronics. For this, the optimal characteristics of the circuit were calculated taking into account the parameters depending on the selected process modes. The calculated value of the critical current of the Josephson junction is $I_c = 5.3\,\mu$A. Optimal process parameters $R_nS = 1000\,\mu m^2$ and junction areas $S = 3.14\,\mu m^2$, are determined allowing to obtain the required critical current.

The manufacturing technology has been worked out, the main parameters of the JPATW elements have been measured, and their compliance with those specified in the design has been demonstrated. Schemes containing separate elements and nodes of JPATW are developed: single SCQIDs and their chains included in coplanar lines. The fabricated structures with JJ demonstrate high quality: $R_j/R_n = 47$, gap 2.88 mV, which enables to create JPATW structures based on such junctions. DC measurements of the test structures showed the difference between the measured parameters and those set. This is due to the dependence of the critical current (I_c) on the size of the junction during direct measurements in an insufficiently shielded system. For HF SCQID chains in the JPATW line, the value of the current jump (I_g) at the slot voltage, which corresponds to the specified values in the structures under study, is more indicative.

Measurements of chains of elements with JJ have demonstrated the fundamental possibility of manufacturing such multielement structures with specified parameters and a small spread of parameters. The possibility of pumping a signal into the SCQID line by passing the pump signal through „grounded“ conductors in a coplanar line has been demonstrated; all this opens up the possibility of implementing JPATW on the basis of the already available niobium technology.

Funding

The study was funded by RSF project No. 21-42-04421, tunnel structures made at the Institute of Radio Engineering and Electronics named after V.A. Kotelnikov of RAS within the scope of the state assignment using unique scientific plant Cryointegral, supported by a grant from the Ministry of Science and Higher Education of Russia, agreement No. 075-15-2021-667.

Conflict of interest

The authors declare that they have no conflict of interest.

References

[1] Quantum squeezing / Eds P.D. Drummond, Z. Ficek. Springer Science & Business Media 27 (2013).

[2] B. Yurke, L.R. Corruccini, P.G. Kaminsky, L.W. Rupp, A.D. Smith, A.H. Silver, R.W. Simon, E.A. Whittaker. Phys. Rev. A **39**, 2519 (1989).

[3] B.Ho Eom, P.K. Day, H.G. LeDuc, J. Zmuidzinas. Nature Phys. **8**, 623 (2012)

[4] K.O. Brien, C. Macklin, I. Siddiqi, X. Zhang. Phys. Rev. Lett. **113**, 157001 (2014).

[5] T.C. White, J.Y. Mutus, I.C. Hoi, R. Barends, B. Campbell, Y. Chen, Z. Chen, B. Chiaro, A. Dunsworth, E. Jeffrey, J. Kelly, A. Megrant, C. Neill, P.J. J.O′Malley, P. Roushan, D. Sank, A. Vainsencher, J. Wenner, S. Chaudhuri, J. Gao, J.M. Martinis. Appl. Phys. Lett. **106**, 242601 (2015).

[6] M.T. Bell, A. Samolov. Phys. Rev. Appl. **4**, 024014 (2015).

[7] C. Macklin, K.O. Brien, D. Hover, M.E. Schwartz, V. Bolkhovsky, X. Zhang, W.D. Oliver, I. Siddiqi. Science **350**, 307 (2015).

[8] A.B. Zorin. Phys. Rev. Appl. **6**, 034006 (2016).

[9] T. Dixon, J.W. Dunstan, G.B. Long, J.M. Williams, P.J. Meeson, C.D. Shelly. Phys. Rev. Appl. **14**, *3*, 034058 (2020).

[10] A.B. Zorin, M. Khabipov, J. Dietel, R. Dolata. 16th Int. Supercond. Electron. Conf. (ISEC), 1 (2017).
[11] A. Miano, O.A. Mukhanov. IEEE Trans. Appl. Supercond. **29**, *5*, 1501706 (2019).
[12] O. Kiselev, M. Birk, A. Ermakov, L. Filippenko, H. Golstein, R. Hoogeveen, N. Kinev, B. van Kuik, A. de Lange, G. de Lange, P. Yagoubov, V. Koshelets. IEEE Trans. Appl. Supercond. **21**, 612–615 (2011).
[13] S. Butz. Supercond. Sci. Tech. **26**, *9*, 094003 (2013).
[14] M.I. Faley, E.A. Kostyurina, K.V. Kalashnikov, Y.V. Maslennikov, V.P. Koshelets, R.E. Dunin-Borkowski. Sensors, **17**, 2798 (2017).

Editor Yu.E. Kitaev